

## ENHANCED POWER LAW AGGLOMERATE GROWTH IN THE FREE MOLECULE REGIME

M. K. WU and S. K. FRIEDLANDER\*

Chemical Engineering Department, University of California, Los Angeles, Los Angeles, CA 90024, U.S.A.

(Received 1 July 1992; accepted 14 October 1992)

**Abstract**—Aerosols generated at high temperatures tend to form agglomerates which can be characterized by a power law exponent, similar to a fractal dimension. The coagulation dynamics of these particles can be described by a modified collision kernel for the free molecule regime. The collision kernel for power law (fractal-like) particles is a homogeneous function, and the equation is solved using self-preserving size distribution theory for fractal dimensions between 2 and 3.

The effects of fractal dimension and primary particle size on agglomerate growth and the size distribution are very strong. Agglomerate growth is rapid at low fractal dimension and fine primary particle size, because the collision cross-section is much larger for the same agglomerate mass. The effect of primary particle size on the rate of particle growth becomes more significant with decreasing fractal dimension, and the particle size distribution becomes much broader at low fractal dimensions.

### NOMENCLATURE

$a$	collision integral (equation (12))
$A$	dimensionless scaling constant (equation (1))
$D_c$	critical dimension
$D_f$	power law exponent or fractal-like dimension (equation (1))
$k$	Boltzmann constant
$Kn$	Knudsen number
$m$	mass fraction
$M$	particle mass
$n$	particle number density
$N$	total particle number density
$N_0$	initial total particle number density
$N_p$	number of primary particles
$q$	growth exponent (equation (20))
$r$	particle radius
$r_0$	primary particle radius
$r_{ij}$	collision distance (equation (4))
$\bar{r}$	radius of the number average volume
$t$	time
$T$	temperature
$v$	particle volume
$v_0$	primary particle volume
$\bar{v}$	number average volume
$X$	random number
$z$	growth exponent (equation (18))

#### Greek letters

$\beta_{ij}$	collision kernel (equation (3))
$\eta$	dimensionless volume (equation (8))
$\lambda$	degree of homogeneity (equation (6))
$\mu_k$	$k$ th moment of the size distribution (equation (14))
$\rho$	particle density
$\phi$	volumetric particle loading (equation (9))
$\psi(\eta)$	dimensionless size distribution function (equation (8))

### INTRODUCTION

Theoretical studies of coagulation in the free molecule regime are frequently based on the assumption of instantaneous and complete coalescence, resulting in the formation of

\* Author to whom correspondence should be addressed.

spherical particles (Lai *et al.*, 1972; Lee *et al.*, 1984). However, agglomerates generated at high temperatures often form irregular structures that can be characterized by a power law exponent ( $D_f$ ) which is less than the classical value of three (Forrest and Witten, 1979; Samson *et al.*, 1987; Schaefer and Hurd, 1990). This exponent has been termed a fractal-like dimension by some investigators, drawing an analogy with fractal concepts (Cleary *et al.*, 1990). The power law exponent influences agglomerate growth dynamics because of the effects of agglomerate morphology on collision diameter.

Although there have been many numerical studies using kinetic growth models of agglomerate formation (Meakin, 1987), uncertainty remains concerning the underlying physical phenomena which give rise to fractal-like particle structures. Mulholland *et al.* (1988) simulated cluster agglomeration in the free molecule regime by solving the Langevin equation and assuming a sticking coefficient of unity, and obtained values of  $D_f$  between 1.89 and 2.07. Some experimental studies agree with this result. Forrest and Witten (1979) studied agglomerates of iron, zinc and silicon dioxide and estimated  $D_f$  to be between 1.7 and 1.9. Similar values have been calculated for soot particles (Megaridis and Dobbins, 1990; Samson *et al.*, 1987; Zhang *et al.*, 1988) and fumed silica (Schaefer and Hurd, 1990). Other investigators have obtained results for  $D_f$  which are greater than the theoretical value. Schmidt-Ott (1988) measured  $D_f$  of silver agglomerates *in situ* by comparing radii before and after tempering, and found that  $D_f = 2.18$ . Matsoukas and Friedlander (1991) generated metal oxide particles in a flame. By studying agglomerate growth dynamics, they found that agglomerate growth was consistent with  $D_f = 2.5$ .

The differences among experimental values of  $D_f$  may result from a number of factors. Estimation methods for  $D_f$  which rely on examining two-dimensional projections of three-dimensional agglomerates are based on the assumption that  $D_f \leq 2$ . Pao *et al.* (1990) showed that the fractal dimension of a two-dimensional projection is not the same as that of a three-dimensional cluster. It is not possible to measure  $D_f > 2$  using methods which measure the radius of gyration. Other factors which can influence  $D_f$  include a sticking coefficient less than unity, restructuring after agglomerates come into contact with each other, or distortion during sampling and subsequent handling, none of which can be easily determined from micrographs. The variety of phenomena which affect agglomerate morphology makes it difficult to interpret experimentally estimated fractal dimensions in terms of theoretical mechanisms.

In this paper we expand upon the theoretical analysis of Matsoukas and Friedlander (1991) for the dynamics of agglomerate growth by systematically examining the effects of  $D_f$  and primary particle size on the shape of the size distribution and the average particle size. The coagulation model is based on the classical collision kernel for Brownian coagulation in the free molecule regime with a modification to account for the fractal-like dimension.  $D_f$  is considered to be simply a constant empirical parameter. It does not necessarily represent a fractal dimension, nor does it imply an agglomeration mechanism of the type used in kinetic growth models. Treating  $D_f$  in this way recognizes that coagulation in the free molecule regime may not result in a unique value of  $D_f$ , and that  $D_f$  may be dependent on experimental conditions and material properties (Schmidt-Ott, 1988). The solution method is the theory of the self-preserving size distribution (Friedlander, 1977). Self-preserving size distributions are asymptotic forms which are approached at long times after the formation of primary particles. They are independent of the initial primary particle size distribution, which in this analysis is assumed to be monodisperse.

#### COAGULATION IN THE FREE MOLECULE REGIME

The basic relationship for a power law (fractal-like) agglomerate can be expressed as follows:

$$N_p = \frac{v}{v_0} = A \left( \frac{r}{r_0} \right)^{D_f}, \quad (1)$$

where  $r_0$  is the radius of a primary particle,  $v_0$  is primary particle volume ( $= 4\pi r_0^3/3$ ),  $N_p$  is

the number of primary particles in an agglomerate,  $v$  is the volume of solids in an agglomerate, and  $r$  is a characteristic agglomerate radius, for example, radius of gyration or collision radius. The dimensionless constant  $A$  depends on the definition of agglomerate radius, fractal dimension and agglomeration mechanism (Wu and Friedlander, 1993).

Agglomerates are fractal-like in a statistical sense. Equation (1) is applicable to the average radius of many agglomerates of the same mass and primary particle size, but not to the radius of an individual agglomerate. Agglomerates are not true fractals, as they are not infinitely scale invariant. The lower limit on the size of an agglomerate is the primary particle ( $N = 1$ ). Fractal concepts generally cannot be applied to agglomerates composed of small numbers of primary particles, because individual primary particles (which have  $D_f = 3$ ) influence  $D_f$  and large scale ( $r \gg r_0$ ) behavior is not exhibited. The use of equation (1) thus implies that  $r \gg r_0$ , i.e., clusters are composed of many primary particles.

It is assumed that  $D_f$  is a constant. Many numerical simulations of coagulation processes show that fractal dimension changes very slowly with cluster size (Tolman and Meakin, 1989). Matsoukas and Friedlander (1991) and Zhang *et al.* (1988) found in experiments that  $D_f$  did not vary significantly over a range of residence times.  $D_f$  is typically found to be between 1.7 and 2.5.

The rate of decay of particle number is:

$$\frac{dN}{dt} = -\frac{1}{2} \int_0^\infty \int_0^\infty \beta_{ij} n_i n_j dv_i dv_j, \quad (2)$$

where  $N$  is the particle number density,  $\beta_{ij}$  is the collision kernel for particles of size  $i$  and  $j$ , and  $n_i$  and  $v_i$  are the number density and volume, respectively, of size  $i$ . The form of the collision kernel depends on the coagulation mechanism. Brownian coagulation in the free molecule regime occurs when the particle size is much smaller than the mean free path ( $Kn > 10$ ). The collision kernel is:

$$\beta_{ij} = \left( \frac{8\pi kT}{M_i} + \frac{8\pi kT}{M_j} \right)^{1/2} r_{ij}^2, \quad (3)$$

where  $M$  is the particle mass and  $r_{ij}$  is the collision distance. When  $D_f > 2$ , the collision distance (Mulholland *et al.*, 1988) is:

$$r_{ij} = r_i + r_j. \quad (4)$$

The characteristic particle size used in this study is agglomerate collision diameter. A major uncertainty in the use of equation (1) to describe agglomerate size is the value of the constant  $A$ . Wu and Friedlander (1993) found that  $A$  is approximately 1 for the radius of gyration and mobility diameter, but depends on the details of the coagulation mechanism. Mulholland *et al.* (1988) suggested that the collision radius of free molecule clusters ( $D_f \sim 2$ ) is 21% greater than the radius of gyration. In the analysis which follows we assume  $A = 1$  to simplify calculations. This assumption can be corrected as better information becomes available on the relationships among different characteristic radii.

Substituting equations (1) and (4) with  $A = 1$  into equation (3), the collision kernel for particles obeying a power law relationship becomes:

$$\beta_{ij} = \left( \frac{6kT}{\rho} \right)^{1/2} \left( \frac{3}{4\pi} \right)^\lambda r_0^{2-6/D_f} \left( \frac{1}{v_i} + \frac{1}{v_j} \right)^{1/2} \left( v_i^{1/D_f} + v_j^{1/D_f} \right)^2 \quad (5)$$

where the degree of homogeneity is:

$$\lambda = \frac{2}{D_f} - \frac{1}{2}. \quad (6)$$

Equation (5) may not be valid for collisions of a large particle with a small particle. Hagenlocher and Friedlander (1989) showed that the collision distance for collisions between point particles and DLA (Diffusion Limited Aggregation) clusters is a function of  $Kn$  (based on primary particle size) as well as  $D_f$ . In this paper it is assumed that the collision distance

scales with  $D_f$  only. Since the collision rate between large agglomerates and primary particles is high (Meesters and Ernst, 1987), the supply of primary particles is rapidly depleted. The effect of Kn is thus only important during the early stages of coagulation. Equation (5) is also not valid for  $D_f < 2$  in the free molecule regime. Mulholland *et al.* (1988) and Jullien and Meakin (1989) have proposed alternative forms for the collision kernel in this range.

The classical theory of irreversible coagulation (Friedlander, 1977) may not be valid at long times below a critical dimension ( $D_c$ ). The theory assumes that density fluctuations are so small that collisions can be regarded as occurring at random (mean field assumption). Kang and Redner (1984) found that in the case of a constant collision kernel and  $D_f > D_c = 2$ , the size distribution is consistent with that predicted by the classical theory. However, when  $D_f < D_c$  neither the size distribution nor concentration decay rates of cluster sizes follow predicted forms. Similar results have also been shown for product and sum kernels (Kang *et al.*, 1986), and it has generally been assumed that  $D_c = 2$  for most kernels. However, van Dongen (1989) has suggested that the value of  $D_c$  is actually dependent on the agglomeration mechanism. It must be noted that mean field coagulation theory is still valid at short times for  $D_f < D_c$ . In view of the uncertainty of the long time validity of the classical theory, free molecule coagulation is only analyzed for  $D_f \geq 2$ .

#### CALCULATION OF THE SIZE DISTRIBUTION FUNCTION

Equation (5) is a homogeneous function of the form:

$$f(\alpha i, \alpha j) = \alpha^\lambda f(i, j). \quad (7)$$

This property enables the self-preserving theory (Friedlander, 1977) to be used to solve for the asymptotic size distribution of power-law agglomerates. The self-preserving variables are:

$$\eta = \frac{v}{\bar{v}} \quad (8)$$

$$\psi(\eta) = \frac{n(v)\bar{v}}{N},$$

where  $\eta$  is the dimensionless volume,  $\psi(\eta)$  is a dimensionless size distribution function,  $n(v)$  is the number density of agglomerates of volume  $v$ ,  $N$  is the total number density of agglomerates,  $\bar{v}$  is the number average particle volume:

$$\bar{v} = \frac{\phi}{N} \quad (9)$$

and  $\phi$  is the volume of aerosol material per unit volume of gas (aerosol loading). Aerosol loading is conserved for coagulation in the absence of condensation or deposition.

Equation (2) can be written in terms of the self-preserving variables:

$$\frac{dN}{dt} = -\frac{1}{2}ac\phi^\lambda N^{2-\lambda}, \quad (10)$$

where

$$c = \left(\frac{6kT}{\rho}\right)^{1/2} \left(\frac{3}{4\pi}\right)^\lambda r_0^{(2-6/D_f)}, \quad (11)$$

and the dimensionless collision integral  $a$  is defined:

$$a = \int_0^\infty \int_0^\infty \left(\frac{1}{\eta_i} + \frac{1}{\eta_j}\right)^{1/2} (\eta_i^{1/D_f} + \eta_j^{1/D_f})^2 \psi_i \psi_j d\eta_i d\eta_j. \quad (12)$$

Substituting equations (1) and (9) into equation (10) and integrating, it is found that the

number average volume (Matsoukas and Friedlander, 1991) grows according to:

$$\bar{v} = \left[ v_0^{1-\lambda} + \frac{1-\lambda}{2} ac\phi t \right]^{1/(1-\lambda)}. \quad (13)$$

Equation (13) is valid at long times. The time required to attain self-preserving behavior depends on the system characteristics (Lai *et al.*, 1972), and Matsoukas and Friedlander (1991) have shown that it can be less than 100 ms in a flat flame aerosol generator.

A Monte Carlo method was used to calculate the self-preserving size distribution (Meakin, 1987). The method starts with a list of 10,000 primary particles of unit mass and volume. Pairs of particles are selected at random, and a random number  $X$  between 0 and 1 generated. If  $X \leq \beta_{ij}/\beta_{\max}$ , then the particles are combined into a particle of mass  $i+j$ .  $\beta_{\max}$  is the value of the collision kernel for a collision between the largest particle and the smallest. To avoid depletion of the list, a new particle is created at each successful collision by randomly selecting a particle from the list and copying it to the position left vacant by the collision. This substitution has no effect on the size distribution. The simulation is continued for very many collisions (i.e. for long times, although time was not explicitly calculated), and so that the minimum value of  $\eta (=1/\bar{v})$  is less than 0.001. Test runs for various numbers of collisions were conducted to ensure that the coagulation time was sufficient. Self-preserving size distributions varied between individual runs because of the small number of particles used in the simulations. Calculated distributions from many runs were averaged to reduce statistical uncertainty.

## RESULTS AND DISCUSSION

### Self-preserving size distributions

Figure 1 shows the self-preserving distributions for a range of fractal dimensions. The most significant feature of this graph is that the size distribution becomes broader with decreasing  $D_f$ . The  $k$ th moment of the size distribution is defined:

$$\mu_k = \int_0^\infty \eta^k \psi(\eta) d\eta. \quad (14)$$

Two constraints on the self-preserving size distribution are:

$$\mu_0 = 1, \quad \mu_1 = 1. \quad (15, 16)$$

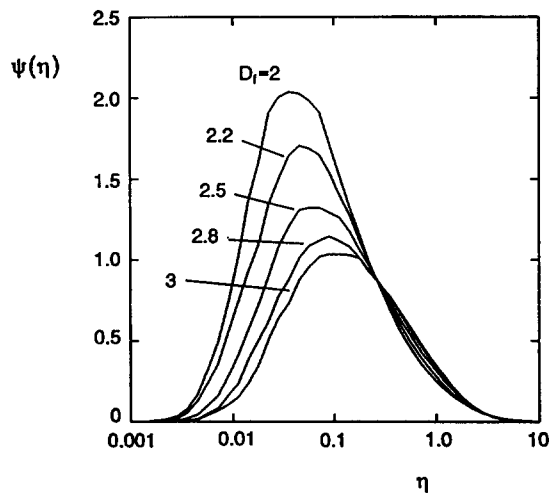


Fig. 1. Self-preserving size distributions. The distributions become broader as  $D_f$  decreases.

Table 1. Properties of the self-preserving size distributions

Property	$D_f$				
	2.0	2.2	2.5	2.8	3.0
$\mu_{1/D_f}$	0.827	0.843	0.867	0.886	0.896
$a$	7.037	6.748	6.607	6.560	6.552

The distributions are normalized to satisfy equation (15), and the first moments (equation (16)) are within 1% of unity.

Values of the  $1/D_f$  moment and the collision integral are listed in Table 1. The number average collision diameter is proportional to the  $1/D_f$  moment (Matsoukas and Friedlander, 1991). The moments for  $D_f = 3$  compare well with those listed in Table 1 of Graham and Robinson (1976), particularly their distribution  $\psi_{LF}(\eta)_{norm}$ , which is the self-preserving size distribution calculated by Lai *et al.* (1972) corrected to satisfy both equations (15) and (16). The differences with the moments of  $\psi_{LF}(\eta)_{norm}$  are less than 1%.

Although the moments show good agreement with previous work, the accuracy of  $\psi(\eta)$  is not believed to be as high. This is due mainly to the statistical nature of the Monte Carlo simulation. The size distribution produced by the simulation was discretized into 40 uniform geometrically-spaced bins in the range  $0.001 < \eta < 10$ . In most runs the size bins at the bottom end of this range contained no agglomerates, resulting in  $\psi(\eta) = 0$ , rather than a small value. Also, the value of  $\psi(\eta)$  for  $\eta$  smaller than the maximum of the distribution is sensitive to the number of agglomerates in the size bins. Statistical differences between runs of the number of agglomerates in these bins resulted in significant variations of  $\psi(\eta)$  in this range. Since the higher moments depend mainly on the upper end of the distribution, inaccuracies in the lower end have only a minor effect. Improved accuracy can be obtained by using a larger number of particles or averaging over a greater number of simulations, but the Monte Carlo technique is computationally time-consuming. In order to obtain self-preserving distributions of greater accuracy and finer discrete size intervals it would be preferable to use another calculation method, such as those of Lai *et al.* (1972) or Graham and Robinson (1976). Monte Carlo simulation is an excellent technique if such precision is not required because of the simplicity of the algorithm.

#### Agglomerate growth

Although results can be expressed in dimensionless form, a dimensional form is used so that predicted particle growth can be more easily related to experimental conditions. The standard conditions used are  $r_0 = 5$  nm,  $\phi = 10^{-8}$ ,  $T = 1500$  K and  $\rho = 2$  g cm $^{-3}$ . While isothermal conditions are assumed, the analysis can be adapted for linear temperature gradients (Matsoukas and Friedlander, 1991).

Industrial aerosol emissions, such as those from coal combustion, frequently have a bimodal size distribution. The coarse mode is composed of non-volatile material, and the fine mode consists of submicrometer particles formed by nucleation and condensation of vapor. If the characteristic diffusion time is long and fine mode loading high, then coagulation of the fine mode can be described approximately by self-preserving theory (Friedlander *et al.*, 1991). The quantity of aerosol in the fine mode is typically in the order of 1% of the total mass produced. Typical values for aerosol loadings of submicrometer particles range between 1 and 400 mg m $^{-3}$  for coal-fired power stations (Lee *et al.*, 1975; McElroy *et al.*, 1982; Schmidt *et al.*, 1976), and 7 mg m $^{-3}$  for a steel plant (Lee *et al.*, 1975). Similar values have been measured in studies of the gas-phase synthesis of metal oxide particles (Akhtar *et al.*, 1991; Steiner, 1992). On a volume basis, aerosol loadings are in the order of  $10^{-7}$  to  $10^{-9}$  m $^3$  of aerosol material per m $^3$  of gas.

Figure 2 shows size distributions for various values of  $D_f$ . The shapes of the size distributions are determined from the self-preserving size distributions with the radius of

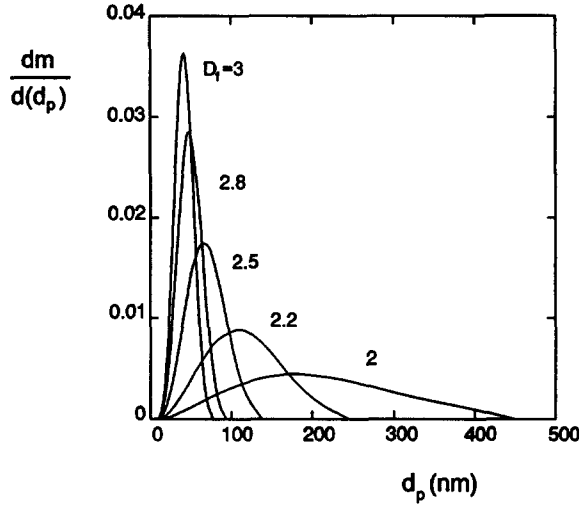


Fig. 2. The size distribution for  $D_f=3$  is narrow, while that for  $D_f=2$  is much broader and includes a high proportion of larger particles. (Results for  $r_0=5$  nm,  $\phi=10^{-8}$ ,  $T=1500$  K,  $\rho=2$  g cm $^{-3}$ ,  $t=0.5$  s.)

the number average volume (average radius) calculated by:

$$\bar{r} = \left[ r_0^{1/z} + \frac{1-\lambda}{2} \left( \frac{6kT}{\rho} \right)^{1/2} \left( \frac{3}{4\pi} \right) r_0^{(3D_f-9)/2} a \phi t \right]^z \quad (17)$$

where the exponent  $z$  is:

$$z = \frac{1}{D_f(1-\lambda)}. \quad (18)$$

(Note that equation (17) corrects an error in equation (12) in the paper by Matsoukas and Friedlander (1991), in which the exponent of  $3/4\pi$  term is written as  $\lambda$  instead of 1. This has no effect on the results and discussion of that paper.)

For the same conditions and residence time, a low value of  $D_f$  results in a broad distribution with a high proportion of mass at large particle sizes. Log-normal size distributions were fitted to the self-preserving size distributions using a non-linear curve-fitting algorithm. The geometric standard deviation is shown in Fig. 3 as a function of  $D_f$ . For  $D_f=3$  a value of  $\sigma_g=1.32$  was obtained. This value has also been reported by Xiong and Pratsinis (1991).

For long times ( $r \gg r_0$ ), agglomerate growth can be approximated by:

$$\begin{aligned} \bar{v} &\propto r_0^{4q/3} (T^{1/2} \phi t)^{1/(1-\lambda)} \\ \bar{r} &\propto r_0^q (T^{1/2} \phi t)^z, \end{aligned} \quad (19)$$

where

$$q = \frac{D_f - 3}{D_f - 4/3}. \quad (20)$$

When  $D_f=3$ , the exponent  $q$  is zero, and agglomerate size is thus independent of the primary particle size. When  $D_f < 3$ ,  $q$  is negative, and for the same values of  $T$ ,  $\phi$  and  $t$ , larger agglomerates are formed from smaller primary particles (Fig. 4). The effect of primary particle size becomes more important with decreasing  $D_f$  because the magnitude of  $q$  increases. When  $D_f \sim 2$ , primary particle size is a major influence on the growth of agglomerates. The mass median diameter used in Figs 4 and 5 is defined as the diameter at which half the mass is contributed by particles smaller than that diameter. It is used here because it incorporates the influence of the agglomerate size distribution, and is experimentally more

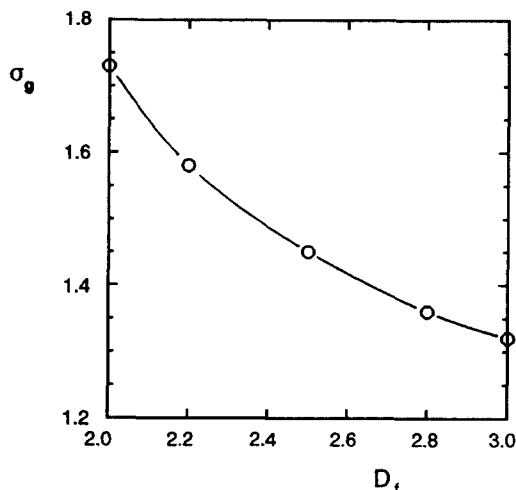


Fig. 3. The geometric standard deviation of the volume-basis self-preserving size distribution decreases with increasing  $D_f$ .

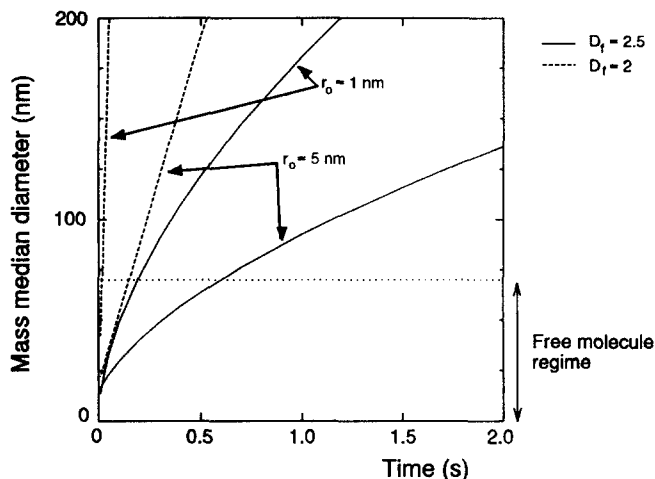


Fig. 4. The mass median diameter is a function of primary particle size for  $D_f < 3$ . A lower value of  $D_f$  and a fine primary particle size results in a higher growth rate. (Results are for  $D_f = 2.5$ ,  $\phi = 10^{-8}$ ,  $T = 1500$  K,  $\rho = 2$  g cm $^{-3}$ .)

meaningful than the average radius. The mass median diameter shows similar behavior as the average radius, which is easily calculated using equation (17) and data in Table 1. The average diameter is smaller than the mass median diameter.  $D_f$  has a strong influence on growth rate (Fig. 5). A low value of  $D_f$  results in agglomerates with open structures which have larger collision cross-sections. Also, the collision integral ( $a$ ) and the exponent  $z$  (equation (18)) increase with decreasing  $D_f$ . The time to reach the self-preserving state decreases with decreasing  $D_f$ . The curves in Figs 4 and 5 are calculated for the free molecule regime, but are extrapolated beyond the limits of this regime.

Average particle size has the same dependence on aerosol loading and residence time. The effect of loading on growth rate depends on  $D_f$  and primary particle size, as shown in Figs 4 and 5. The value of aerosol loading can vary by an order of magnitude from that used in the calculations, and a loading of  $\phi = 10^{-7}$  results in much more rapid growth than depicted in Figs 4 and 5. The effect of temperature is less important, as the exponent in equation (19) is smaller in magnitude.



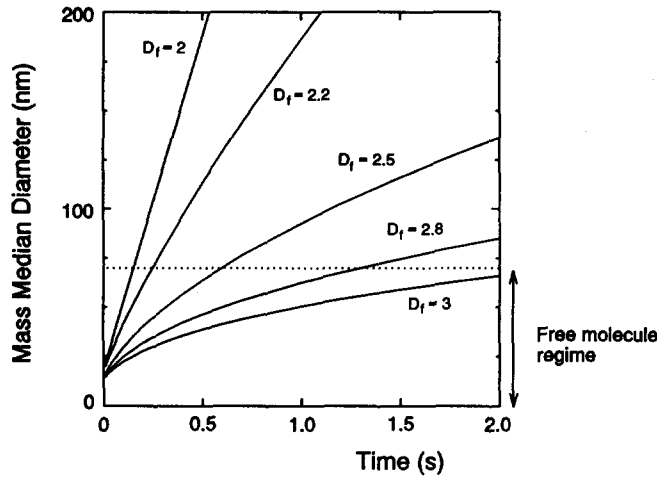


Fig. 5. The growth rate of the mass median diameter is much greater at low values of  $D_f$ , because of the increased collision cross-section. (Results are for  $r_0 = 5$  nm,  $\phi = 10^{-8}$ ,  $T = 1500$  K,  $\rho = 2$  g cm $^{-3}$ .)

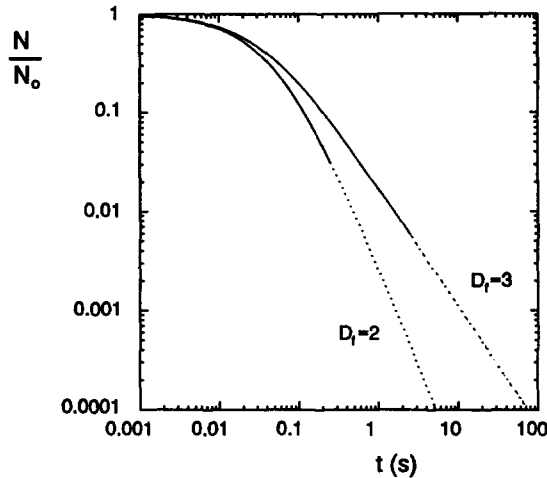


Fig. 6. The decay of particle number density (calculated with equation (21)) rapidly approaches the asymptotic slope of  $-2$  and  $-6/5$  for  $D_f = 2$  and  $D_f = 3$ , respectively. The bold lines represent the free molecule regime. (Results are for  $r_0 = 5$  nm,  $\phi = 10^{-8}$ ,  $T = 1500$  K,  $\rho = 2$  g cm $^{-3}$ .)

The decay of particle number density can be obtained by integrating equation (10):

$$\left(\frac{N}{N_0}\right)^{\lambda-1} = 1 + \frac{(1-\lambda)}{2} ac \phi^\lambda N_0^{1-\lambda} t. \quad (21)$$

As  $t \rightarrow \infty$ ,  $\ln(N/N_0) \propto \ln(t)/(\lambda-1)$ . The slopes of the curves in Fig. 6 approach asymptotic values of  $-2$  and  $-6/5$  for  $D_f = 2$  and  $3$ , respectively after  $0.3$  s. The rapid growth rate at  $D_f = 2$  shown in Fig. 5 is reflected in a large difference in particle number density with  $D_f = 3$ . It may be possible to estimate the fractal dimension of experimentally formed particles by measuring the slope of the particle number concentration decay curve.

## CONCLUSIONS

The growth rate and size distribution of power law agglomerates are strongly influenced by fractal dimension ( $D_f$ ) and primary particle size. An open agglomerate ( $D_f \sim 2$ ) has a larger collision diameter than a solid sphere containing the same mass of material, resulting in much more rapid agglomerate growth. Given the same agglomerate mass,

$D_f$  and temperature history, a fine primary particle size results in a much larger agglomerate than a coarse primary particle size and the growth rate is more rapid. The effect of primary particle size on growth rate becomes more significant at lower  $D_f$ . The particle size distribution becomes broader with decreasing  $D_f$ . It may be possible to make use of the effects of primary particle size and  $D_f$  on particle growth to condition the size distribution and influence the efficiency of gas cleaning devices and the properties of powdered materials.

*Acknowledgements*—Dr Murray Wu wishes to express his appreciation for the support of the Ralph M. Parsons Foundation Fellowship in Pollution Prevention. Professor Sheldon K. Friedlander acknowledges support from the Engineering Research Center for the Control of Hazardous Substances under NSF Grant ECD-9046215.

## REFERENCES

- Akhtar, M. K., Xiong, Y. and Pratsinis, S. E. (1991) *AIChE J.* **37**, 1561–1570.  
 Cleary, T., Samson, R. and Gentry, J. W. (1990) *Aerosol Sci. Technol.* **12**, 518–525.  
 Forrest, S. R. and Witten, T. A., Jr (1979) *J. Phys. A: Math. Gen.* **12**, L109–L117.  
 Friedlander, S. K. (1977) *Smoke, Dust and Haze*. John Wiley, New York.  
 Friedlander, S. K., Koch, W. and Main, H. H. (1991) *J. Aerosol Sci.* **22**, 1–8.  
 Graham, S. C. and Robinson, A. (1976) *J. Aerosol Sci.* **7**, 261–273.  
 Hagenloech, R. and Friedlander, S. K. (1989) *J. Colloid Interface Sci.* **133**, 185–191.  
 Jullien, R. and Meakin, P. (1989) *J. Colloid Interface Sci.* **127**, 265–272.  
 Kang, K. and Redner, S. (1984) *Phys. Rev. A* **30**, 2833–2836.  
 Kang, K., Redner, S., Meakin, P. and Leyvraz, F. (1986) *Phys. Rev. A* **33**, 1171–1182.  
 Lai, F. S., Friedlander, S. K., Pich, J. and Hidy, G. M. (1972) *J. Colloid Interface Sci.* **39**, 395–405.  
 Lee, K. W., Chen, H. and Gieseke, J. A. (1984) *Aerosol Sci. Technol.* **3**, 53–62.  
 Lee, R. E., Jr, Crist, H. L., Riley, A. E. and MacLeod, K. E. (1975) *Envir. Sci. Technol.* **9**, 643–647.  
 Matsoukas, T. and Friedlander, S. K. (1991) *J. Colloid Interface Sci.* **146**, 495–506.  
 McElroy, M. W., Carr, R. C., Ensor, D. S. and Markowski, G. R. (1982) *Science* **215**, 13–19.  
 Meakin, P. (1987). In *Time-Dependent Effects in Disordered Materials* (Edited by Pynn, R. and Riste, T.), pp. 45–70. Plenum Press, New York.  
 Meesters, A. and Ernst, M. H. (1987) *J. Colloid Interface Sci.* **119**, 576–587.  
 Megaridis, C. M. and Dobbins, R. A. (1990) *Combust. Sci. Technol.* **71**, 95–109.  
 Mulholland, G. W., Samson, R. J., Mountain, R. D. and Ernst, M. H. (1988) *Energy Fuels* **2**, 481–486.  
 Pao, J.-R., Chang, Y.-C. and Gentry, J. W. (1990) *J. Aerosol Sci.* **21**, S63–S66.  
 Samson, R. J., Mulholland, G. W. and Gentry, J. W. (1987) *Langmuir* **3**, 272–281.  
 Schaefer, D. W. and Hurd, A. J. (1990) *Aerosol Sci. Technol.* **12**, 876–890.  
 Schmidt, E. W., Gieseke, J. A. and Allen, J. M. (1976) *Atmos. Envir.* **10**, 1065–1069.  
 Schmidt-Ott, A. (1988) *Appl. Phys. Lett.* **52**, 954–956.  
 Steiner, C. K. R. (1992) Metal oxide aerosol formation in high temperature processes. M.S. Thesis, University of California, Los Angeles.  
 Tolman, S. and Meakin, P. (1989) *Phys. Rev. A* **40**, 428–437.  
 van Dongen, P. G. J. (1989) *Phys. Rev. Lett.* **63**, 1281–1284.  
 Wu, M. K. and Friedlander, S. K. (1993) *J. Colloid Interface Sci.*, Submitted.  
 Xiong, Y. and Pratsinis, S. E. (1991) *J. Aerosol Sci.* **22**, 637–655.  
 Zhang, H. X., Sorensen, C. M., Ramer, E. R., Olivier, B. J. and Merklin, J. F. (1988) *Langmuir* **4**, 867–871.